LETTER

doi:10.1038/nature11924

Adult somatic stem cells in the human parasite *Schistosoma mansoni*

James J. Collins III[1,2], Bo Wang[1,3], Bramwell G. Lambrus[1], Marla E. Tharp[1], Harini Iyer[1] & Phillip A. Newmark[1,2]

Schistosomiasis is among the most prevalent human parasitic diseases, affecting more than 200 million people worldwide[1]. The aetiological agents of this disease are trematode flatworms (*Schistosoma*) that live and lay eggs within the vasculature of the host. These eggs lodge in host tissues, causing inflammatory responses that are the primary cause of morbidity. Because these parasites can live and reproduce within human hosts for decades[2], elucidating the mechanisms that promote their longevity is of fundamental importance. Although adult pluripotent stem cells, called neoblasts, drive long-term homeostatic tissue maintenance in long-lived free-living flatworms[3,4] (for example, planarians), and neoblast-like cells have been described in some parasitic tapeworms[5], little is known about whether similar cell types exist in any trematode species. Here we describe a population of neoblast-like cells in the trematode *Schistosoma mansoni*. These cells resemble planarian neoblasts morphologically and share their ability to proliferate and differentiate into derivatives of multiple germ layers. Capitalizing on available genomic resources[6,7] and RNA-seq-based gene expression profiling, we find that these schistosome neoblast-like cells express a fibroblast growth factor receptor orthologue. Using RNA interference we demonstrate that this gene is required for the maintenance of these neoblast-like cells. Our observations indicate that adaptation of developmental strategies shared by free-living ancestors to modern-day schistosomes probably contributed to the success of these animals as long-lived obligate parasites. We expect that future studies deciphering the function of these neoblast-like cells will have important implications for understanding the biology of these devastating parasites.

Although classic studies of cell proliferation in *Schistosoma* focused on reproductive tissues[8,9], occasional 'undifferentiated' somatic cells that incorporated tritiated thymidine in adult parasites were noted. Encouraged that these cells could represent neoblast-like stem cells, we treated adult *S. mansoni* with the thymidine analogue 5-ethynyl-2′-deoxyuridine (EdU)[10] to examine the distribution of S phase cells in the parasite (Fig. 1a, b). In addition to the expected incorporation in the highly proliferative reproductive organs (testes, ovaries and vitellaria) (Fig. 1a, b and Supplementary Fig. 1), we observed a population of EdU$^+$ cells throughout the soma of male and female parasites (Fig. 1a–d). Similar distributions of EdU-incorporating cells were observed whether parasites were given EdU during *in vitro* culture or *in vivo* by intraperitoneal injection of schistosome-infected mice. Analogous to the neoblasts in free-living flatworms[11,12], these proliferating somatic cells (PSCs) were restricted to the mesenchyme of male and female worms (Fig. 1c, d), not associated with reproductive organs, and were often found in clusters near the intestine (Supplementary Fig. 2a). We also observed a conspicuous population of PSCs adjacent to the ventral sucker (Supplementary Fig. 2b). PSCs traversed the cell cycle: they initially expressed the cell-cycle-associated transcript histone h2b (Supplementary Fig. 3a–c) and progressed to M phase within 24 h after an EdU pulse (Supplementary Fig. 3d).

Neoblasts are the only proliferating somatic cells in planarians[4,11] and they possess a distinct morphology: they are round-to-ovoid mesenchymal cells with a high nuclear-to-cytoplasmic ratio, a large nucleolus, and they often extend a cytoplasmic projection[3,11,13]. To determine whether PSCs share similarities with planarian neoblasts, we examined these cells by dissociating male tissues devoid of germ cells (Fig. 1e). In these preparations we observed a number of distinct differentiated cell types that failed to incorporate EdU, including cells with a low nuclear-to-cytoplasmic ratio, neuron-like cells, and ciliated

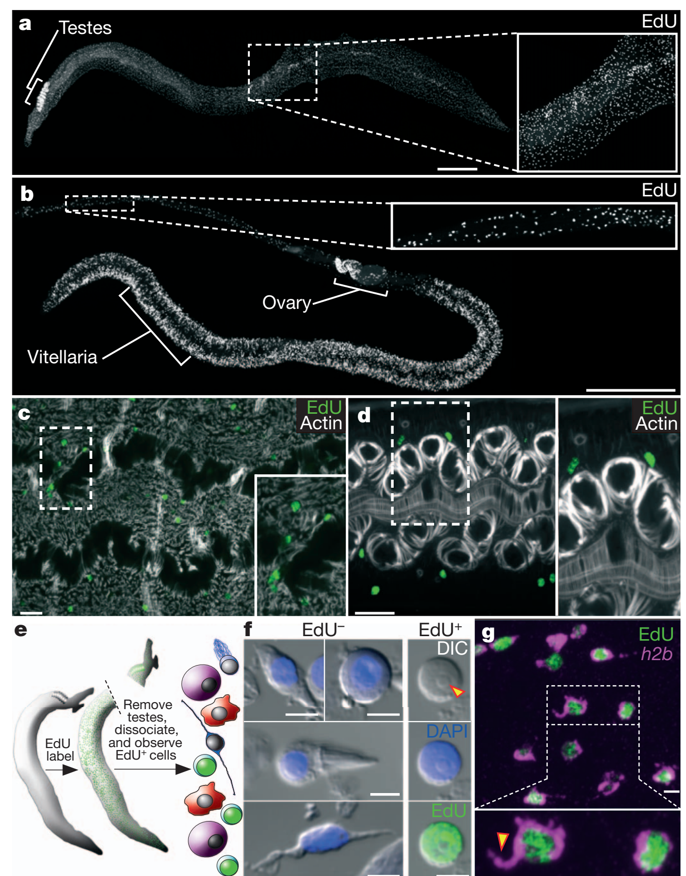

Figure 1 | Proliferation of somatic cells in adult schistosomes. **a**, **b**, EdU labelling in male (**a**) and female (**b**) parasites. **c**, **d**, Distribution of mesenchymal PSCs in male (**c**) and female (**d**) parasites. Phalloidin staining for actin shows male enteric and dorso-ventral muscles and female enteric and uterine muscles. **e**, Strategy to characterize PSC morphology. **f**, The morphology of EdU$^-$ and EdU$^+$ cells. The arrowhead indicates a nucleolus. **g**, FISH for histone h2b with EdU labelling. The arrowhead indicates a cytoplasmic projection. **a**–**d**, **g** are confocal projections; **a**, **b** are derived from tiled stacks. Scale bars: **a**, **b**, 500 μm; **c**, **d**, 20 μm; **f**, **g**, 5 μm. Inset magnifications, relative to original: **a**, **g**, ×2.2; **b**, ×2.6; **c**, ×1.6; **d**, ×1.7.

[1]Howard Hughes Medical Institute and Department of Cell and Developmental Biology, University of Illinois at Urbana-Champaign, Urbana, Illinois 61801, USA. [2]Neuroscience Program, University of Illinois at Urbana-Champaign, Urbana, Illinois 61801, USA. [3]Institute for Genomic Biology, University of Illinois at Urbana-Champaign, Urbana, Illinois 61801, USA.

©2013 Macmillan Publishers Limited. All rights reserved

cells (Fig. 1f). By contrast, we found that EdU incorporation was restricted to a neoblast-like population of cells with scant cytoplasm ($n = 136$ out of 137 cells) and often a prominent nucleolus (Fig. 1f). We also inspected PSCs within the mesenchyme using EdU to label nuclei and fluorescent *in situ* hybridization (FISH) to detect histone h2b messenger RNA in the cytoplasm of proliferative cells. Consistent with our results from tissue macerates, EdU$^+$ cells possess a narrow rim of cytoplasm surrounding their nucleus, and these cells often display a cytoplasmic projection (Fig. 1g). These observations highlight morphological similarities between proliferating cells in schistosomes and planarian neoblasts.

Previous studies have exploited the sensitivity of planarian neoblasts to γ-irradiation as a means to identify neoblast-enriched transcripts[14–16]. Using this strategy to identify PSC-expressed genes, we exposed parasites to various dosages of γ-irradiation and determined that 100–200 Gy were sufficient to block EdU incorporation (Fig. 2a). Because of their high ratio of somatic tissue to reproductive tissue and their large number of PSCs relative to female worms (compare insets in Fig. 1a and b), our remaining studies, unless otherwise noted, focused on male parasites. By comparing the transcriptional profiles of irradiated and non-irradiated parasites by RNA-seq (Fig. 2b), we identified 128 genes with significantly downregulated expression ($\geq$2-fold, $P < 0.05$) 48 h after irradiation (Fig. 2c and Supplementary Table 1). Highlighting the efficacy of this approach to identify transcripts specific to proliferating cells, we found that genes expressed in differentiated tissues, such as the intestine (*S. mansoni* cathepsin B (ref. 17)), were unaffected by irradiation. By contrast, our list of downregulated genes was enriched for factors involved in the cell cycle (Supplementary Fig. 4 and Supplementary Table 1).

In addition to identifying cell-cycle-associated factors, systematic comparison of irradiation-sensitive genes with neoblast-enriched transcripts[14,15,18,19] uncovered a number of interesting similarities (Supplementary Table 1). For instance, homologues of genes known to regulate planarian neoblasts such as *p53*, a sox-family transcription factor, fibroblast growth factor receptors, and argonaute 2 (*ago2*)[14,20–22], were significantly downregulated in irradiated schistosomes (Supplementary Fig. 4 and Supplementary Table 1). Another distinctive feature of neoblasts[3,14,22], and the somatic stem cells of other invertebrates[23], is that they often express post-transcriptional regulators associated with germline development (for example, *vasa*, *piwi*, *tudor* and *nanos*). Although *vasa*-like genes have been reported in *Schistosoma*, no true *vasa* orthologue has been indentified[24]. Similarly, *piwi* and *tudor* genes seem to be absent from schistosomes (data not shown). However, we identified a *nanos* orthologue (*S. mansoni nanos-2* (*Smnanos-2*)) that was downregulated in somatic tissue after irradiation (Supplementary Fig. 4 and Supplementary Table 1). Because these genes represented potential regulators of PSC behaviour and could serve as useful markers for these cells, we examined their expression by whole-mount *in situ* hybridization. We detected *Smago2-1*, *Smnanos-2* and *SmfgfrA* transcripts in cells scattered throughout the mesenchyme (Fig. 2d and Supplementary Fig. 5) in a pattern similar to that of cells incorporating EdU (Fig. 1a). This mesenchymal expression was radiation sensitive (Fig. 2d), indicating that these genes are expressed in proliferating cells. Consistent with

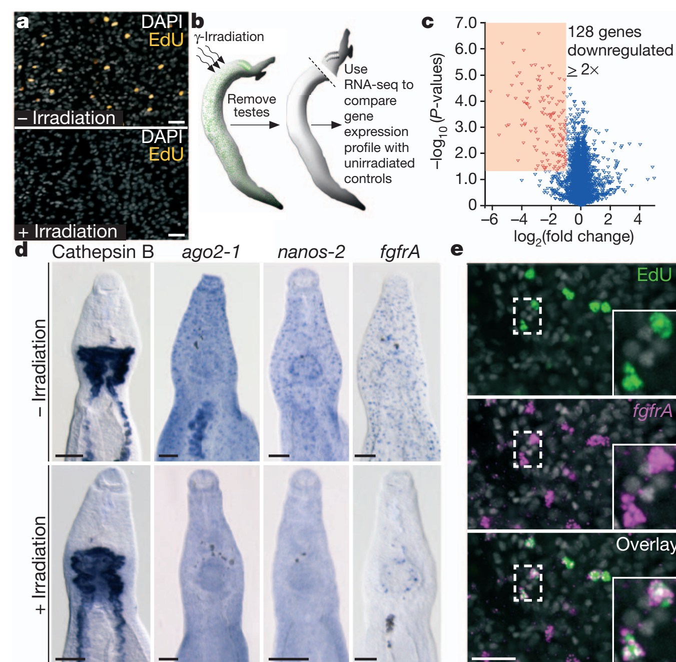

Figure 2 | Transcriptional profiling identifies genes expressed in proliferative cells. **a**, EdU incorporation is abrogated at d3 after irradiation. **b**, Strategy to identify PSC-expressed genes. **c**, Volcano plot showing expression differences in control versus irradiated parasites. $n = 3$ for each group. **d**, Whole-mount *in situ* hybridization for various transcripts in unirradiated and d5 post-irradiation parasites. $n > 3$ parasites. **e**, EdU labelling and FISH for *SmfgfrA*. A total of 1,988 out of 2,000 EdU$^+$ PSCs were *SmfgfrA*$^+$ after a 20–22-h pulse ($n = 20$ male parasites). **a**, **e** are confocal projections. Scale bars: **a**, **e**, 20 μm; **d**, 100 μm. Inset magnification, relative to original: **e**, ×2.6.

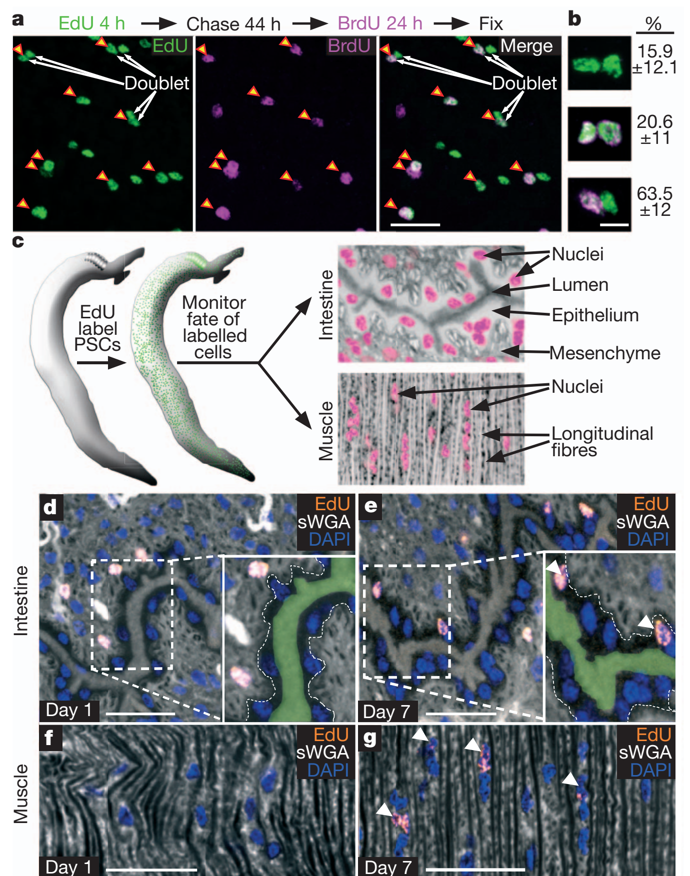

Figure 3 | PSCs self-renew and differentiate. **a**, EdU and BrdU double labelling. Arrowheads indicate EdU$^+$BrdU$^+$ nuclei. Arrows indicate EdU$^+$ 'doublets'. **b**, Percentage (±s.d.) EdU$^+$ doublets (green) that are BrdU$^-$–BrdU$^-$ (top), BrdU$^+$–BrdU$^+$ (middle, BrdU is magenta), or BrdU$^+$–BrdU$^-$ (bottom). $n = 21$ parasites. **c**, Strategy to monitor cellular differentiation. **d–g**, EdU and succinylated wheat germ agglutinin (sWGA) labelling showing EdU$^+$ cells in male intestine (**d**, **e**) or dorsal musculature (**f**, **g**) at d1 (**d**, **f**) and d7 (**e**, **g**) following a pulse. Insets in **d**, **e**, show intestinal basal surface (dashed lines) and lumen (green). Arrowheads in **e** and **g** show EdU$^+$ intestinal cells (**e**) or muscle cells (**g**). Images are confocal projections. Scale bars: **a**, **d–g**, 20 μm; **b**, 5 μm. Inset magnifications, relative to original: **d**, **e**, ×1.5.

©2013 Macmillan Publishers Limited. All rights reserved

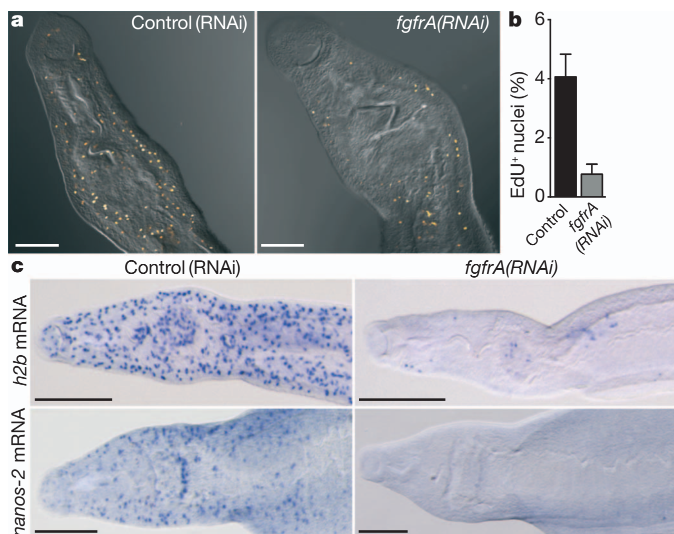

Figure 4 | *SmfgfrA* is required for the maintenance of somatic stem cells. **a**, EdU labelling and DIC images in control and *SmfgfrA(RNAi)* parasites at RNAi d17. **b**, Percentage of EdU^+ nuclei/total nuclei in dissociated tissues from control (RNAi) ($n = 3{,}002$ nuclei) and *SmfgfrA(RNAi)* ($n = 3{,}642$ nuclei) parasites. Error bars indicate 95% confidence intervals, $P < 0.0001$ χ^2. **c**, Whole-mount *in situ* hybridization for histone h2b (top row) and *Smnanos-2* (bottom row) transcripts in control (left column) versus *SmfgfrA(RNAi)* (right column) parasites at RNAi d20–21. $n > 5$ parasites per experiment. Scale bars: **a**, 100 μm; **c**, 200 μm.

this idea, we found that after an EdU pulse, >99% of EdU-incorporating somatic cells also expressed *SmfgfrA* (Fig. 2e).

To determine whether PSCs are stem cells, we assessed their ability both to self-renew and to produce differentiated cell types. To examine self-renewal, we administered sequential pulses of EdU and 5-bromo-2′-deoxyuridine (BrdU) to parasites *in vitro*. Because nearly all PSCs that incorporate EdU are $SmfgfrA^+$, the ability of EdU^+ cells to incorporate BrdU in subsequent cell cycles would suggest that $fgfrA^+$ PSCs self-renew (that is, divide and produce more $fgfrA^+$ PSCs). For these experiments we chose a chase period of 44 h, as this time frame should give many EdU^+ PSCs sufficient time to divide (Supplementary Fig. 3d). Consistent with PSCs possessing the capacity for self-renewal, we found that 41% of cells that initially incorporate EdU are $BrdU^+$ 3 days after an initial EdU pulse (Fig. 3a). Furthermore, we observed that many EdU^+ cells were distributed in pairs, or 'doublets' (Fig. 3a); we suggest that most of these doublets are the products of cell division (Supplementary Discussion and Supplementary Fig. 6). In these EdU^+ doublets, a disproportionately large fraction displayed asymmetric BrdU incorporation (that is, one nucleus is EdU^+BrdU^+, whereas the other is EdU^+BrdU^-) (Fig. 3b and Supplementary Discussion). This observation suggests that division progeny have an asymmetric capacity to proliferate. Whether this represents stem-cell-like asymmetric division or temporal differences in the ability of these cells to re-enter the cell cycle requires further experimentation. Nevertheless, these data are consistent with PSCs (or some PSC subpopulation) being capable of self-renewal.

To examine the capacity of PSCs to differentiate, we performed EdU pulse–chase experiments *in vivo*. For these experiments, schistosome-infected mice were injected with EdU and the distribution of EdU^+ cells was monitored at early (day (d) 1) and late (d7) time points (Fig. 3c). We successfully used this pulse–chase approach to monitor the differentiation of schistosome germ cells (Supplementary Fig. 7). Visualizing the syncytial epithelium of the schistosome intestine at d1, we did not observe EdU^+ intestinal nuclei in male or female parasites (Fig. 3d, 0 EdU^+/3,151 $DAPI^+$ nuclei, 14 mixed sex parasites, $n = 5$ mice), confirming that cells in the intestine do not proliferate. After a 7-day chase, however, ~2.5% of the intestinal nuclei were EdU^+ (Fig. 3e, 56 EdU^+/2,189 $DAPI^+$ nuclei, 10 mixed sex parasites, $n = 3$ mice). This observation suggests that cells initially labelled with EdU have the capacity to migrate into the intestine and differentiate into new intestinal cells. Similarly, we were able to monitor the differentiation of new cells in the body wall muscles. At d1 no EdU^+ nuclei were observed in the male body wall musculature (Fig. 3f, 0 EdU^+/1,882 $DAPI^+$ nuclei, 13 male parasites, $n = 6$ mice), whereas at d7 ~10% of the muscle cell nuclei were EdU^+ (Fig. 3g, 55 EdU^+/584 $DAPI^+$ nuclei, 6 male parasites, $n = 3$ mice). Because virtually all cells that initially incorporate EdU are $SmfgfrA^+$, we suggest that these double-positive cells probably represent the only source of new intestinal and muscle cells and, thus, represent a collectively multipotent population of neoblast-like stem cells. Whether all $SmfgfrA^+$ PSCs are multipotent or whether they exist as lineage-restricted progenitors remains unclear.

Although progress has been made in identifying transcriptional[14] and post-transcriptional[22] regulators of planarian neoblasts, little is known about the signal transduction networks functioning within these cells. Because the expression of FGF receptor family members in proliferative cells is conserved between planarians[14,21] and schistosomes, we speculated that FGF signalling could regulate these cells in *S. mansoni*. To examine this idea, we disrupted *SmfgfrA* in *in vitro*-cultured adult parasites using RNA interference (RNAi) (Supplementary Fig. 8). We found that inhibition of *SmfgfrA* resulted in reduced EdU incorporation (Fig. 4a, b and Supplementary Table 2) and down-regulation of cell-cycle-associated transcripts (Fig. 4c and Supplementary Fig. 8). To resolve whether this effect is due to reduced cell proliferation or a failure to maintain neoblast-like cells, we monitored the expression of PSC markers *Smago2-1* and *Smnanos-2* in *SmfgfrA(RNAi)* parasites. *SmfgfrA* RNAi treatment resulted in a marked reduction in the number of cells expressing *Smnanos-2* (Fig. 4c) as well as significantly reduced mRNA levels for *Smago2-1* and *Smnanos-2* (Supplementary Fig. 8b). Together, these results indicate that *SmfgfrA* promotes the long-term maintenance of neoblast-like cells in *S. mansoni*. FGF signalling is known to influence multiple processes, such as cell proliferation, differentiation and survival; furthermore, it has key roles in various stem-cell populations[25]. Our results suggest a conserved role for FGF signalling in controlling stem-cell behaviour in these parasites and demonstrate the feasibility of using RNAi to abrogate adult gene expression and manipulate neoblast-like cells in *S. mansoni*.

Adult schistosomes can modulate growth in response to host immune signals[26] and male–female pairing status[2,27] and they can regenerate damaged tissues after sublethal doses of the anti-schistosomal drug praziquantel[28]. These observations reveal the developmental plasticity of schistosomes, and suggest that these parasites can use distinct developmental programs in response to a range of external stimuli. Future studies characterizing the role of neoblast-like cells in diverse contexts could address long-standing gaps in our knowledge of schistosome biology and may reveal novel therapeutic strategies for treating and eliminating schistosomiasis.

METHODS SUMMARY

EdU detection in adult parasites was performed using Alexa 488 azide (Invitrogen) as described previously[10]. To observe the morphology of PSCs, single-cell suspensions were obtained by incubating minced male parasites in trypsin-EDTA (Sigma); cell suspensions were fixed in 4% formaldehyde and spread on microscope slides. For *in situ* hybridizations, parasites were fixed in 4% formaldehyde for 4.5 h and processed essentially as described previously[29]. Immunofluorescence and histological staining were performed similar to previous studies[30]. For transcriptional profiling, male parasites were γ-irradiated, cultured *in vitro* for 48 h and processed for RNA-seq (Illumina). Transcriptional differences between irradiated and mock-irradiated controls were assessed using CLC Genomics Workbench (version 4, CLC Bio). For RNAi, *in vitro* cultured parasites were soaked with dsRNA (20–30 μg ml^{-1}) freshly added on days 1–3 and every 5–6 days thereafter. A 1.5-kb dsRNA derived from an irrelevant bacterial sequence was used as a negative control. Experiments with and care of vertebrate animals were performed in accordance with protocols approved by the Institutional Animal Care and Use

©2013 Macmillan Publishers Limited. All rights reserved

Committee (IACUC) of the University of Illinois at Urbana-Champaign (protocol approval number 10035).

Full Methods and any associated references are available in the online version of the paper.

Received 3 September 2012; accepted 18 January 2013.
Published online 20 February 2013.

1. Chitsulo, L., Engels, D., Montresor, A. & Savioli, L. The global status of schistosomiasis and its control. *Acta Trop.* **77,** 41–51 (2000).
2. Basch, P. F. *Schistosomes: Development, Reproduction, and Host Relations* (Oxford Univ. Press, 1991).
3. Wagner, D. E., Wang, I. E. & Reddien, P. W. Clonogenic neoblasts are pluripotent adult stem cells that underlie planarian regeneration. *Science* **332,** 811–816 (2011).
4. Newmark, P. A. & Sánchez Alvarado, A. Not your father's planarian: a classic model enters the era of functional genomics. *Nature Rev. Genet.* **3,** 210–219 (2002).
5. Brehm, K. *Echinococcus multilocularis* as an experimental model in stem cell research and molecular host-parasite interaction. *Parasitology* **137,** 537–555 (2010).
6. Protasio, A. V. *et al.* A systematically improved high quality genome and transcriptome of the human blood fluke *Schistosoma mansoni*. *PLoS Negl. Trop. Dis.* **6,** e1455 (2012).
7. Berriman, M. *et al.* The genome of the blood fluke *Schistosoma mansoni*. *Nature* **460,** 352–358 (2009).
8. Den Hollander, J. E. & Erasmus, D. A. *Schistosoma mansoni*: DNA synthesis in males and females from mixed and single-sex infections. *Parasitology* **88,** 463–476 (1984).
9. Nollen, P. M., Floyd, R. D., Kolzow, R. G. & Deter, D. L. The timing of reproductive cell development and movement in *Schistosoma mansoni, S. japonicum*, and *S. haematobium,* using techniques of autoradiography and transplantation. *J. Parasitol.* **62,** 227–231 (1976).
10. Salic, A. & Mitchison, T. J. A chemical method for fast and sensitive detection of DNA synthesis *in vivo*. *Proc. Natl Acad. Sci. USA* **105,** 2415–2420 (2008).
11. Newmark, P. A. & Sánchez Alvarado, A. Bromodeoxyuridine specifically labels the regenerative stem cells of planarians. *Dev. Biol.* **220,** 142–153 (2000).
12. Forsthoefel, D. J., Park, A. E. & Newmark, P. A. Stem cell-based growth, regeneration, and remodeling of the planarian intestine. *Dev. Biol.* **356,** 445–459 (2011).
13. Baguñá, J. & Romero, R. Quantitative analysis of cell types during growth, degrowth and regeneration in the planarians *Dugesia mediterranea* and *Dugesia tigrina*. *Hydrobiologia* **84,** 181–194 (1981).
14. Wagner, D. E., Ho, J. J. & Reddien, P. W. Genetic regulators of a pluripotent adult stem cell system in planarians identified by RNAi and clonal analysis. *Cell Stem Cell* **10,** 299–311 (2012).
15. Solana, J. *et al.* Defining the molecular profile of planarian pluripotent stem cells using a combinatorial RNAseq, RNA interference and irradiation approach. *Genome Biol.* **13,** R19 (2012).
16. Eisenhoffer, G. T., Kang, H. & Sánchez Alvarado, A. Molecular analysis of stem cells and their descendants during cell turnover and regeneration in the planarian *Schmidtea mediterranea*. *Cell Stem Cell* **3,** 327–339 (2008).
17. Caffrey, C. R., McKerrow, J. H., Salter, J. P. & Sajid, M. Blood 'n' guts: an update on schistosome digestive peptidases. *Trends Parasitol.* **20,** 241–248 (2004).
18. Önal, P. *et al.* Gene expression of pluripotency determinants is conserved between mammalian and planarian stem cells. *EMBO J.* **31,** 2755–2769 (2012).
19. Labbé, R. M. *et al.* A comparative transcriptomic analysis reveals conserved features of stem cell pluripotency in planarians and mammals. *Stem Cells* **30,** 1734–1745 (2012).
20. Pearson, B. J. & Sánchez Alvarado, A. A planarian p53 homolog regulates proliferation and self-renewal in adult stem cell lineages. *Development* **137,** 213–221 (2010).
21. Ogawa, K. *et al.* Planarian fibroblast growth factor receptor homologs expressed in stem cells and cephalic ganglions. *Dev. Growth Differ.* **44,** 191–204 (2002).
22. Rouhana, L., Shibata, N., Nishimura, O. & Agata, K. Different requirements for conserved post-transcriptional regulators in planarian regeneration and stem cell maintenance. *Dev. Biol.* **341,** 429–443 (2010).
23. Juliano, C. & Wessel, G. Versatile germline genes. *Science* **329,** 640–641 (2010).
24. Skinner, D. E. *et al.* *Vasa*-like DEAD-box RNA helicases of *Schistosoma mansoni*. *PLoS Negl Trop Dis* **6,** e1686 (2012).
25. Lanner, F. & Rossant, J. The role of FGF/Erk signaling in pluripotent cells. *Development* **137,** 3351–3360 (2010).
26. Davies, S. J. *et al.* Modulation of blood fluke development in the liver by hepatic $CD4^+$ lymphocytes. *Science* **294,** 1358–1361 (2001).
27. Severinghaus, A. E. Sex studies on *Schistosoma japonicum*. *Q. J. Microsc. Sci.* **71,** 653–702 (1928).
28. Shaw, M. K. & Erasmus, D. A. *Schistosoma mansoni:* structural damage and tegumental repair after *in vivo* treatment with praziquantel. *Parasitology* **94,** 243–254 (1987).
29. Collins, J. J. III *et al.* Genome-wide analyses reveal a role for peptide hormones in planarian germline development. *PLoS Biol.* **8,** e1000509 (2010).
30. Collins, J. J. III, King, R. S., Cogswell, A., Williams, D. L. & Newmark, P. A. An atlas for *Schistosoma mansoni* organs and life-cycle stages using cell type-specific markers and confocal microscopy. *PLoS Negl. Trop. Dis.* **5,** e1009 (2011).

Supplementary Information is available in the online version of the paper.

Acknowledgements We thank R. Roberts-Galbraith, M. Issigonis and L. Rouhana for comments on the manuscript; R. King for sharing the cathepsin B plasmid and unpublished protocols; and A. Hernandez for assistance with Illumina sequencing. Schistosome-infected mice were provided by the NIAID Schistosomiasis Resource Center and the Biomedical Research Institute through NIAID contract no. HHSN272201000005I. This work was supported by: NIH F32 HD062124 (J.J.C.) and NIH R21 AI099642 (P.A.N.). P.A.N. is an investigator of the Howard Hughes Medical Institute.

Author Contributions J.J.C., B.W., B.G.L., M.E.T. and H.I. performed experiments. J.J.C. and B.W. analysed data. J.J.C. and P.A.N. designed the study and wrote the paper.

Author Information RNA-seq analyses have been deposited in the NCBI Gene Expression Omnibus under accession number GSE42757. Reprints and permissions information is available at www.nature.com/reprints. The authors declare no competing financial interests. Readers are welcome to comment on the online version of the paper. Correspondence and requests for materials should be addressed to P.A.N. (pnewmark@life.illinois.edu).

©2013 Macmillan Publishers Limited. All rights reserved

METHODS

Parasite acquisition and culture. Adult *S. mansoni* (6–8 weeks after infection) were obtained from infected mice by hepatic portal vein perfusion[31] with 37 °C DMEM (Mediatech) plus 5% fetal calf serum (FBS, Hyclone/Thermo Scientific Logan). Parasites were rinsed several times in DMEM + 5% FBS and cultured (37 °C/5% CO_2) in Basch's Medium 169 (ref. 32) and 1× antibiotic-antimycotic (Gibco/Life Technologies). Media was changed every 1–3 days.

EdU labelling. For *in vitro* labelling, parasites were cultured in Basch's Medium 169 supplemented with 10 μM EdU (Invitrogen) diluted from a 10 mM stock in DMSO. Unless otherwise noted, animals were pulsed for 18–24 h. For *in vivo* labelling, schistosome-infected mice (6–8 weeks after infection) were given a single intraperitoneal injection (100–200 mg EdU per kg body weight) with 5 mg ml^{-1} EdU dissolved in PBS and then collected at various time points after injection.

***In situ* hybridization.** Male and female parasites were separated by incubation (2–3 min) in a 0.25% solution of the anaesthetic ethyl 3-aminobenzoate methanesulphonate (Sigma-Aldrich) dissolved in Basch's Medium 169 or phosphate buffered saline (PBS). Relaxed parasites were then killed in a 0.6 M solution of $MgCl_2$ and fixed for 4.5 h in 4% formaldehyde dissolved in PBSTx (PBS + 0.3% Triton X-100). After fixation, parasites were dehydrated in MeOH and stored at −20 °C. Samples were rehydrated by incubation in 1:1 MeOH:PBSTx followed by incubation in PBSTx. Rehydrated samples were bleached for 1–2 h in formamide bleaching solution (0.5% Formamide, 0.5% SSC, and 1.2% H_2O_2), rinsed with PBSTx, treated with proteinase K (2–10 μg ml^{-1}, Invitrogen) for 20–30 min at room temperature and post-fixed for 10–15 min in 4% formaldehyde in PBSTx. Samples were hybridized at 52–55 °C and otherwise processed as previously described[29,33]. Plasmids used for riboprobe synthesis were generated as described previously[29] using oligonucleotide primers listed in Supplementary Table 3.

Immunofluorescence, histological staining and EdU detection. Parasites were relaxed, killed, fixed, dehydrated and rehydrated as described above and bleached in 6% H_2O_2 dissolved in PBS for 0.5–2 h. Dehydration and bleaching were omitted for samples labelled with phalloidin. Samples were then treated with Proteinase K and post-fixed as described above. Immunofluorescence, lectin and phalloidin staining were performed as described previously[30]. Rabbit anti-phospho-histone H3 Ser 10 (anti-pH3) (D2C8, Cell Signaling), rhodamine-conjugated sWGA (Vector Laboratories), and Alexa Fluor 568 phalloidin (Invitrogen) were used at 1:1,000, 1:100 and 1:100, respectively. EdU detection was performed essentially as previously described[10,34] with 100 μM Alexa Fluor 488 or Alexa Fluor 594 azide conjugates. All imaging was performed as described previously[29,30]. To quantify intestinal cell differentiation, the number of EdU^+ and $DAPI^+$ intestinal nuclei were determined from 12 consecutive confocal sections imaged from the intestine. To quantify muscle cell differentiation, the number of EdU^+ and $DAPI^+$ nuclei were determined from 4 to 9 consecutive confocal sections through the dorsal muscle layer of male parasites.

Tissue dissociation and EdU detection. After an overnight pulse with 10 μM EdU, the heads and testes of adult male *S. mansoni* were removed and the remaining tissue added to dissociation solution (Hanks Balanced Salt Solution with 3.5× trypsin-EDTA (from 10× stock, Sigma-Aldrich)) and minced with a razor blade. These tissue fragments were incubated in ~4 ml of dissociation solution for 45–60 min at room temperature on a rocker and gentle pipetting was used to break up large tissue fragments. This mixture was passed over two sets of cell strainers (100 and 40 μm, BD) and dissociated cells were collected by centrifugation (250*g* for 5 min). Pelleted cells were fixed in 4% formaldehyde in PBS for 30 min, spotted on Superfrost Plus microscope slides (Fisher Scientific), permeabilized for 30 min with PBSTx, and EdU was detected as described above with 10 μM Alexa Fluor 488 azide.

To quantify the ratio of EdU^+ to total $DAPI^+$ nuclei in RNAi knockdowns, eight male parasites were processed as above and tiled images of EdU and DAPI labelling were captured on a Zeiss LSM 710 (Plan-Apochromat 20x/0.8). Numbers of EdU^+ and $DAPI^+$ nuclei were quantified using the Image-based Tool for Counting Nuclei (ITCN) plugin for ImageJ[35].

γ-Irradiation and transcriptional profiling. Parasites (d43 after infection) were collected from mice, suspended in Basch medium 169, and exposed to 200 Gy of γ-irradiation using a Gammacell-220 Excel with a Co^{60} source (Nordion). Control parasites were mock irradiated. Parasites were cultured in Basch Medium 169 and 48 h after irradiation males were separated from female parasites using ethyl 3-aminobenzoate methanesulphonate. After separation, the head and testes of males were removed and purified total RNA was prepared from the remaining tissue from pools of 14–18 parasites using Trizol (Invitrogen) and DNase treatment (DNA-free RNA kit, Zymo Research). Three independent biological replicates were performed for both control and irradiated experimental groups. Individually tagged libraries for RNA-seq were prepared (TruSeq RNaseq Sample prep kit, Illumina), pooled in a single lane, and 100-bp reads were generated using an Illumina HiSeq2000. Library preparation and Illumina sequencing were performed at the W.M. Keck Center for Comparative and Functional Genomics. The resulting reads were mapped to the annotated *S. mansoni* genome[6] (v5.0) and differences in gene expression were determined using CLC Genomics Workbench (CLC bio). Statistical enrichment of Gene Ontology terms was determined in CLC Genomics Workbench using a hyper geometric test that is similar to the GOstat test described in previous studies[36]. To examine similarities between proteins encoded from irradiation-sensitive transcripts in *S. mansoni* and genes expressed in planarian neoblasts, we compared our schistosome data set with both neoblast-enriched and 'whole' transcriptomes[14,15,18,19] using standalone tBLASTn. Schistosome proteins sharing no similarity to translated planarian mRNAs (*e*-value cutoff $>1 \times 10^{-5}$) were omitted from analysis. Assignment of whether protein pairs were orthologous, homologous, paralogous, or unrelated was assessed manually on an individual basis. Data and evidence supporting protein similarity are provided in Supplementary Table 1.

EdU/BrdU double labelling. Parasites labelled with 10 μM EdU and BrdU were fixed in Methacarn (6:3:1 methanol:chloroform:glacial acetic acid) or processed for *in situ* hybridization. After a 45-min 2N HCl treatment, EdU was detected and parasites were processed for anti-BrdU immunofluorescence (anti-BrdU 1:500, clone MoBU, Invitrogen). We observed no crossreactivity between this antibody and EdU.

To quantify the level of BrdU/EdU overlap and measure centre-to-centre distances between nuclei, three-dimensional confocal stacks from EdU/BrdU-labelled animals were re-sampled to give isotropic voxels, and subjected to Gaussian filtering and background-subtraction. Labelled nuclei were segmented with Imaris (Bitplane Inc.) using parameters empirically determined to minimize the need for manual corrections; typically, fewer than 5% of the total nuclei required correction. The three-dimensional coordinates of the nuclei were exported and analysed with MATLAB. Overlapping EdU- and BrdU-labelled nuclei were defined as nuclei with centre-to-centre distances <1 nuclear size (~4 μm). Statistical analyses were performed in Origin (OriginLab).

RNA interference. Although procedures have been previously described[37,38], RNAi experiments with adult parasites were based on methods optimized for schistosomula[39]. Briefly, *in vitro* cultured parasites were soaked with 20–30 μg of dsRNA freshly added on days 1–3 and every 5–6 days thereafter. As a negative control, animals were soaked with dsRNA synthesized from the *ccdB* and *camR*-containing insert of pJC53.2 (ref. 29). dsRNA synthesis was performed as previously described[29]. Sequences used to generate dsRNAs are provided in Supplementary Fig. 9. To measure mRNA levels, total RNA from control and knockdown parasites (~8 male posterior somatic fragments) was reverse transcribed (iScript cDNA Synthesis kit, Bio-Rad) and quantitative real-time PCR was performed on an Applied Biosystems Step One Plus instrument using GoTaq qPCR Master Mix with SYBR green (Promega). Transcript levels were normalized to the mRNA levels of proteasome subunit beta type-4 (smp_056500). Relative quantities were calculated using the ΔΔCt calculation in the Step One Plus software. Oligonucleotide primer sequences are listed in Supplementary Table 3.

31. Lewis, F. Schistosomiasis. *Curr. Protoc. Immunol.* Ch. 19, Unit 19 11 (2001).
32. Basch, P. F. Cultivation of *Schistosoma mansoni in vitro*. I. Establishment of cultures from cercariae and development until pairing. *J. Parasitol.* **67,** 179–185 (1981).
33. Cogswell, A. A., Collins, J. J. III, Newmark, P. A. & Williams, D. L. Whole mount *in situ* hybridization methodology for *Schistosoma mansoni*. *Mol. Biochem. Parasitol.* **178,** 46–50 (2011).
34. Neef, A. B. & Luedtke, N. W. Dynamic metabolic labeling of DNA *in vivo* with arabinosyl nucleosides. *Proc. Natl Acad. Sci. USA* **108,** 20404–20409 (2011).
35. Abramoff, M. D., Magelhaes, P. J. & Ram, S. J. Image processing with ImageJ. *Biophotonics Int.* **11,** 36–42 (2004).
36. Falcon, S. & Gentleman, R. Using GOstats to test gene lists for GO term association. *Bioinformatics* **23,** 257–258 (2007).
37. Skelly, P. J., Da'dara, A. & Harn, D. A. Suppression of *cathepsin B* expression in *Schistosoma mansoni* by RNA interference. *Int. J. Parasitol.* **33,** 363–369 (2003).
38. Boyle, J. P., Wu, X. J., Shoemaker, C. B. & Yoshino, T. P. Using RNA interference to manipulate endogenous gene expression in *Schistosoma mansoni* sporocysts. *Mol. Biochem. Parasitol.* **128,** 205–215 (2003).
39. Štefanić, S. *et al.* RNA interference in *Schistosoma mansoni* schistosomula: selectivity, sensitivity and operation for larger-scale screening. *PLoS Negl. Trop. Dis.* **4,** e850 (2010).

©2013 Macmillan Publishers Limited. All rights reserved